α-Homo-DNA and RNA Form a Parallel Oriented Non-A, Non-B-Type Double Helical Structure

Matheus Froeyen,[a] Eveline Lescrinier,[a] Luc Kerremans,[a] Helmut Rosemeyer,[b] Frank Seela,[b] Birgit Verbeure,[a] Irene Lagoja,[a] Jef Rozenski,[a] Arthur Van Aerschot,[a] Roger Busson,[a] and Piet Herdewijn*[a]

Abstract: Cross-talking between nucleic acids is a prerequisite for information transfer. The absence of observed base pairing interactions between pyranose and furanose nucleic acids has excluded considering the former type as a (potential) direct precursor of contemporary RNA and DNA. We observed that α-pyranose oligonucleotides (α-homo-DNA) are able to hybridize with RNA and that both nucleic acid strands are parallel oriented. Hybrids between α-homo-DNA and DNA are less stable. During the synthesis of α-homo-DNA we observed extensive conversion of N^6-benzoyl-5-methylcytosine into thymine under the usual deprotection conditions of oligonucleotide synthesis. α-Homo-DNA:RNA represents the first hybridization system between pyranose and furanose nucleic acids. The duplex formed between α-homo-DNA and RNA was investigated using CD, NMR spectroscopy, and molecular modeling. The general rule that orthogonal orientation of base pairs prevents hybridization is infringed. NMR experiments demonstrate that the base moieties of α-homo-DNA in its complex with RNA, are equatorially oriented and that the base moieties of the parallel RNA strand are pseudoaxially oriented. Modeling experiments demonstrate that the duplex formed is different from the classical A- or B-type double stranded DNA. We observed 15 base pairs in a full helical turn. The average interphosphate distance in the RNA strand is 6.2 Å and in the α-homo-DNA strand is 6.9 Å. The interstrand P–P distance is much larger than found in the typical A- and B-DNA. Most helical parameters are different from those of natural duplexes.

Keywords: α-homo-DNA · base-pair orientation · DNA recognition · oligonucleotides · RNA

Introduction

Although all naturally occurring nucleic acids have not been analyzed with respect to their configurational uniformity, natural α-oligonucleotides have not been identified. However, nucleosides with an α-ribose moiety have been isolated from natural sources, that is 1-(α-D-ribofuranosyl)-5,6-dimethyl-benzimidazole,[1] α-NAD,[2] and α-adenosine.[3] Studies on prebiotic synthesis demonstrate that when a dry mixture of adenine and ribose in the presence of Mg^{2+} and inorganic polyphosphate was heated for two hours at 100 °C, α-adenosine and β-adenosine are formed in a 1:1 ratio (total yield 8%).[4] This demonstrates that the likelihood of formation of both anomers under presumed prebiotic conditions is equal. The extensive work on the evaluation of α-oligonucleotides for antisense purposes was preceded by the first synthesis of dinucleoside monophosphates containing α-nucleosides by A. Holy[5] and U. Séquin.[6] Using simple Dreiding stereomodels, U. Séquin predicted that oligonucleotides consisting of α-nucleotide units might be able to hybridize with complementary β-strand in a parallel way.[7] He concluded that "the replication of genetic material might also have proceeded with α-nucleotides". Experimentally it was demonstrated that α-deoxyribonucleotides hybridize in a parallel way with their β-counterpart.[8, 9] RNase H is not able to degrade RNA in an α-oligodeoxyribonucleotide:RNA duplex.[10, 11] α-Deoxynucleosides preferentially adopt the S-type sugar conformation, as a result of a cooperative stereoelectronic effect of nucleobase and 3′-hydroxyl group.[12] ^{1}H NMR studies of an α-oligodeoxynucleotide annealed to its β-complement demonstrate that the conformation of the parallel duplex belongs to the right-handed B family and that the sugar moieties in the α- and β-strand adopt the C2′-endo puckering conformation.[8, 13, 14] α-Oligonucleotides targeted to the cap site of rabbit β-globin mRNA reduce

[a] Prof. P. Herdewijn, Dr. M. Froeyen, Dr. E. Lescrinier, Dr. L. Kerremans, A. B. Verbeure, Dr. I. Lagoja, Prof. J. Rozenski, Prof. A. Van Aerschot, Prof. R. Busson
Laboratory of Medicinal Chemistry
Rega Institute for Medical Research
Minderbroedersstraat 10, 3000 Leuven (Belgium)
Fax: (+32) 16-337340
E-mail: piet.herdewijn@rega.kuleuven.ac.be

[b] Dr. H. Rosemeyer, Prof. F. Seela
Laboratory of Organic Chemistry
Osnabrück University, Barbarastrasse 7
4500 Osnabrück (Germany)

 © WILEY-VCH Verlag GmbH, D-69451 Weinheim, 2001 0947-6539/01/0723-5183 $ 17.50+.50/0

protein synthesis in a dose-dependent manner.[15] Other modified α-oligonucleotides which are able to form duplexes with natural nucleic acids are α-phosphorothioates,[16, 17] oligo-α-D-bicyclodeoxynucleotides,[18] α-(P-NH_2)phosphor-amidates,[19] α-*N*-alkylphosphoramidates,[20] α-(N3′→P5′)phosphoramidates,[21] α-methylphosphonates,[22] 5-propynyl-α-oligonucleotide,[23] α-LNA,[24] and α-L-ribo-LNA.[25, 26] The conclusion of this research is that a wide variety of α-furanose-oligonucleotides are able to hybridize with β-furanose oligonucleotides in both the deoxyribose (DNA) and ribose (RNA) series and that both strands are parallel oriented. In one exception [oligo-α-$(dT)_8$:oligo-β-$(rA)_8$] antiparallel annealing was described.[27] The configuration at the anomeric center in furanose oligonucleotides is likely to be decisive for the strand orientation but not for the selectivity in the hybridization with DNA and RNA.

Investigations on pyranose nucleosides are inspired by the search on nucleic acid alternatives which possess a potentially natural type of molecular structure (i.e., a sugar moiety belonging to the family of aldo sugars) and the ability for informational base pairing in the Watson–Crick mode.[28] β-Homo-DNA or oligo(2′,3′-dideoxy-β-D-glucopyranosyl) nucleotides is an artificial oligonucleotide which was used as a model system for the study of the family of hexopyranosyl oligonucleotides.[29] β-Homo-DNA shows stronger Watson–Crick base pairing than DNA and RNA and has a base-pairing system which is orthogonal to that of the natural systems.[26] β-Homo-DNA does not cross-pair with DNA.[29, 30] α-Homo-DNA, however, has not been thoroughly studied, so far. We previously observed that α-homo-DNA-thymidylate does not hybridize with natural oligodeoxyadenylate;[31] this was attributed to the conformational preference of the α-dideoxyhexopyranose nucleoside. 1-(2,3-Dideoxy-*erythro*-α-D-hexopyranosyl)thymine crystallizes in the $^1C_4$ conformation with an equatorially oriented heterocyclic base and axially oriented 4′-hydroxyl and 5′-hydroxymethyl moiety (Scheme 1).[32] Based on our experiences with hexitol nucleic

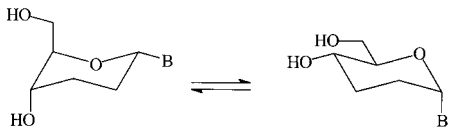

Scheme 1. Conformational equilibrium of 2,3-dideoxy-*erythro*-α-D-hexopyranosyl nucleoside. The thymine nucleoside crystallizes in the $^1C_4$ conformation.

acids,[33] the absence of hybridization between α-homo-DNA-oligothymidylate and DNA-oligoadenylate can be explained by the wrong preorganization of the α-homo-DNA oligomer (the hexitol nucleoside bases are oriented orthogonally to the bases of α-hexopyranose nucleosides). However, we did not have any experimental evidence to confirm this hypothesis. Here, we investigated the potential base pairing between α-homo-DNA and β-D-deoxyribonucleic acids and β-D-ribonucleic acids of mixed sequences. This study was inspired by our observations that a) the conformation of a nucleoside may be different before and after incorporation in an oligonucleotide,[34] and b) several modified oligonucleotides discriminate between DNA and RNA for their pairing properties,[35, 36] and c) results obtained with polyA:polyT hybrids are not good models for the study of mixed-sequence duplexes.

Results and Discussion

Synthesis of nucleosides: The 2,3-dideoxy-D-glucopyranosyl nucleosides with a thymine, N^4-benzoylcytosine, and adenine base moiety are obtained as minor products during the Lewis acid catalyzed condensation reaction between methyl 4,6-di-*O*-acyl-2,3-dideoxy-α-D-glucopyranoside[37] or 3,4,6-tri-*O*-acetyl-D-glucal[30] and the silylated nucleobases. In the latter example, condensation is followed by hydrogenation of the 2′,3′-double bond. The α-/β-mixture of the nucleoside with an N^6-benzoyladenine base moiety is difficult to separate.[37] The α-isomer could be enriched in solution by the crystallization of a substantial part of the β-isomer.[37] Complete separation of both anomers was carried out after 6′-*O*-monomethoxytritylation. The 5-methyl-N^6-benzoylcytosine analogue was synthesized from the thymine nucleoside using literature procedures.[38] The structure of 1-(2,3-dideoxy-*erythro*-α-D-hexopyranosyl)thymine was confirmed by X-ray diffraction analysis.[32] Monomethoxytritylation of the primary hydroxyl group, followed by activation of the secondary hydroxyl group into a phosphoramidite (Figure 1), allowed us to synthesize

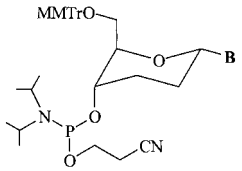

B
thymine
N^6-benzoyladenine
N^4-benzoyl-5-methylcytosine
N^4-benzoylcytosine

Figure 1. Structure of the phosphoramidite building blocks used for the synthesis of α-homo-DNA.

several oligonucleotides which sequences are depicted in Table 1. As determined using ^{1}H NMR spectroscopy,[37] 1-(4,6-di-*O*-acetyl-2,3-dideoxy-α-D-*erythro*-hexopyranosyl)thymine and 1-(4,6-di-*O*-acetyl-2,3-dideoxy-α-D-*erythro*-hexopyranosyl)-N^6-benzoylcytosine adopt a conformation with an equatorial base moiety, and so does 1-(2,3-dideoxy-α-D-*erythro*-hexopyranosyl)-5-methyl-N^6-benzoylcytosine. This is in accordance with published results describing the X-ray analysis of the thymine congener.[32] The equatorial position of the base in the α-anomer infers a pyranose nucleoside in the $^1C_4$ conformation instead of the usual $^4C_1$ conformation. Apparently, the occurrence of this conformation is driven by the

Table 1. Molecular masses of 2,3-dideoxy-α-D-hexopyranosyl-containing oligonucleotides measured by electrospray mass spectrometry.

Sequence or composition	Monoisotopic mass	Mass found
α-h($TC^{Me}TC^{Me}C^{Me}T$)	1981.5	1981.6
α-h($T_4C^{Me}_2$)	1982.5	1982.7
α-h(T_5C^{Me})	1983.5	1983.6
α-h($TC^{Me}TC^{Me}C^{Me}TC^{Me}TC^{Me}C^{Me}C^{Me}T$)	3885.9	3886.4
α-h(T_{13})	4210.8	4211.3

© WILEY-VCH Verlag GmbH, D-69451 Weinheim, 2001
0947-6539/01/0723-5184 $ 17.50+.50/0 *Chem. Eur. J.* **2001**, *7*, No. 23

steric influence of the nucleobase and is opposite to the conformation that would have been expected based on the steric effect of the hydroxymethylene group and on the dominant influence of the anomeric effect. Rather surprisingly, however, in the case of 1-(6-*O*-monomethoxytrityl-2,3-dideoxy-α-D-*erythro*-hexopyranosyl)-N^6-benzoyladenine, the base moiety is axially oriented and both 4′- and 6′-substituents are equatorially oriented.

This immediately follows from the rather small vicinal coupling constant between H1′ and both H2′ hydrogens, so that in the ^{1}H NMR spectrum the H1′ signal appears as a triplet, corresponding to an equatorial hydrogen. It thus seems that in the case of purines as the base moiety, the conformation of the sugar does not change from $^4C_1$ to $^1C_4$ in going from the β to the α-anomer as it does within the pyrimidine series.

This conclusion was also confirmed by the observation of a similar small coupling (and thus equatorially positioned hydrogen) for H1′ of 9-(2,3-dideoxy-α-D-glucopyranosyl)-N^2-isobutyryl-guanine[37] (compound **22** in that report).

Oligonucleotide synthesis and mass spectrometric analysis: The synthesis of α-homo-DNA was performed in the same way as the regular DNA synthesis with similar coupling yields. However, when benzoyl protected 5-methylcytosine nucleosides were incorporated, and deprotection was carried out using ammonia in H_2O, several peaks were observed when running an anion-exchange HPLC analysis at pH 12. These oligomers were isolated and analyzed using mass spectrometry. These data can be interpreted by the conversion of one or several 5-methylcytosine bases in thymine residues. Oligonucleotides, in which a single C^{Me} to T conversion took place, would have a molecular ion one mass unit higher; a double conversion would lead to an increase of two mass units. Although it is possible to deduce the sequence of oligonucleotides from CAD mass spectra, it was not applicable in this case because the fragmentation behavior does not follow the rules known for DNA or RNA. Instead, the relative numbers of C^{Me} and T residues were assessed from the intensities of the signals for the base anion losses from CAD data for α-h($TC^{Me}TC^{Me}C^{Me}T$) (see Figure 2). The doubly charged ion $[M-2H]^{2-}$ was selected as precursor and the collision energy was set high enough (150 eV) to release all the bases. For the oligonucleotide containing three C^{Me} and three T residues we found a relative intensity of 24.4 % for the base anion $[C^{Me}]^-$. Assuming that the base anion intensity depends on its structure and is proportional with the number of bases, relative intensities of $(24.4/3\times2)/(100/3\times4)\times100\,\% = 12.2\,\%$ and $(24.4/3\times1)/(100/3\times5)\times100\,\% = 4.9\,\%$ are expected for one and two conversions of C^{Me} to T, respectively. The experimental values 14.2 and 5.8 are in good agreement with the theoretical values. Similar conversions of C^{Me} to T were observed for the 12-mer.

We previously observed that upon base protection of 5-methylcytosine with an acyl group, the equilibrium shifts in the direction of the 4-imino tautomer.[39] By treatment in basic conditions, both N^4-debenzoylation as well as hydrolysis of the 4-imino function can be expected (Scheme 2). This observation warrants for a careful control of oligonucleotide integrity when the *N*-benzoyl group is used as protecting group for the 5-methylcytosine base moiety. In this case, we isolated the oligomers with the correct mass and used them for the hybridization studies. All other oligonucleotides show the correct mass as shown in Table 1.

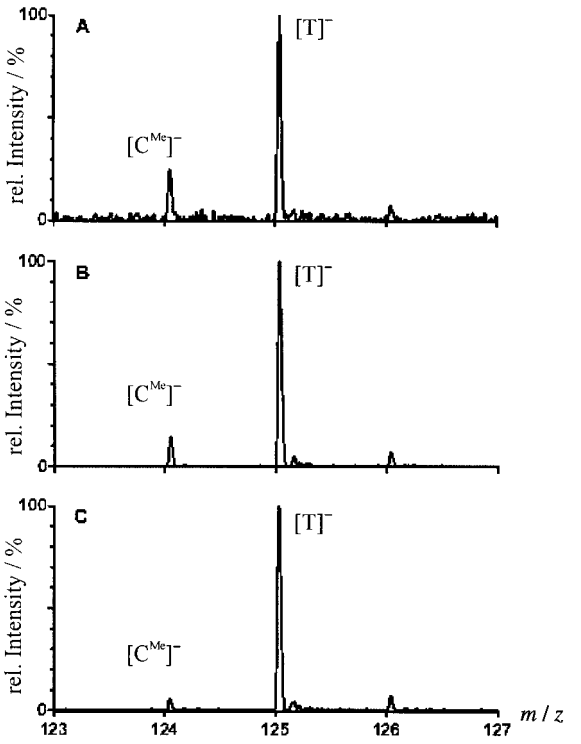

Figure 2. Parts of the collisionally activated dissociation mass spectra for A): α-h($TC^{Me}TC^{Me}C^{Me}T$), B): α-h($T_4C^{Me}_2$), and C): α-h(T_5C^{Me}) showing the loss of the base anions from the oligonucleotides. The $[C^{Me}]^-/[T]^-$ intensity ratio follows the base content in the oligonucleotides.

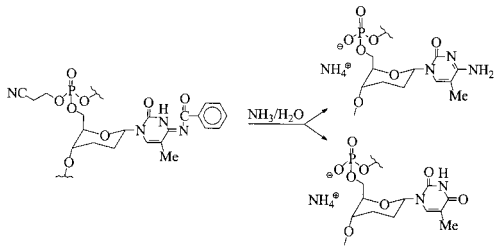

Scheme 2. Deprotection of N^4-benzoyl-5-methylcytosine bases using concentrated ammonia partially leads to thymine formation as side reaction.

Thermal stability studies: α-Homo-oligoT and α-homo-oligoA do not form stable complexes with their DNA complement at 0.1 M NaCl (Table 2). However, α-homo-$(A)_{13}$ hybridizes with oligo$(dT)_{13}$ at 1 M NaCl. α-Homo-oligoT and α-homo-oligoA are able to form duplexes with RNA. Likewise, α-homo-oligonucleotides demonstrate self pairing as a complex formed between α-h$(T)_{13}$ and α-h$(A)_{13}$ has a T_m of 23.8 °C at 0.1 M NaCl. The stability of these duplexes is comparable to the stability of regular d$(T)_{13}$:r$(A)_{13}$ and r$(U)_{13}$:r$(A)_{13}$ duplexes (T_m: 26 °C) and is dependent on the salt concentration. α-Homo-oligoA does not self associate as no T_m is observed when heating a solution of single stranded α-homo-oligoA. The T_m of the α-homo-oligoA:α-homo-oligoT association and

Table 2. T_m values of α-homo-DNA complexes and reference duplexes of natural nucleic acids.[a]

α-homo-DNA (6′→4′)	DNA complement		RNA complement	
	0.1 M NaCl	1.0 M NaCl	0.1 M NaCl	1.0 M NaCl
α-h$(T)_{13}$	NM	NM	28.0	37.0
α-h$(A)_{13}$	NM	28.5	22.8	40.2
α-h(TC^{Me}TC^{Me}C^{Me}T)				
antiparallel	ND	NM	ND	NM
parallel	ND	ND	24.0	28.4
α-h(TC^{Me}TC^{Me}C^{Me}TC^{Me}TC^{Me}C^{Me}C^{Me}T)				
antiparallel	NM	NM	49.6	58.5
parallel	26.2	33.1	67.3	72.1
DNA/RNA (5′→3′)	**DNA complement**		**RNA complement**	
	0.1 M NaCl	1.0 M NaCl	0.1 M NaCl	1.0 M NaCl
d$(T)_{13}$	ND	ND	32.2	42.4
d$(A)_{13}$	ND	ND	13.9	35.2
d(TCTCCTCTCCCT)				
antiparallel	50.0	58.0	64.0	72.9
parallel	32.7	45.0	49.4	60.1
d(AGGGAGAGGAGA)				
antiparallel	ND	ND	47.0	ND
r(UCUCCUCUCCCU)				
antiparallel	ND	ND	72.0	ND
parallel	ND	ND	56.2	ND

[a] Melting temperature [°C] were determined at 260 nm, pH 7.5 (20 mM KH_2PO_4, 0.1 mM EDTA) with a concentration of 4 μM of each oligonucleotide; NM: no melting curve observed; ND: not determined.

of α-homo-oligoA:r$(U)_{13}$ is nearly the same. Likewise, mixed pyrimidine sequences of α-homo-DNA hybridize with their RNA complement and this as well for a 6-mer as for a 12-mer. With the 12-mer also weak hybridization with the DNA complement is observed. Similar RNA selective hybridization properties are described with, for example, L-ribonucleic acids.[35] Hybridization is observed between [(L)-dU]$_{20}$ and poly(rA) and between [(L)-rU]$_{12}$ and poly(rA). Neither [(L)-dU]$_{20}$ nor [(L)-rU]$_{12}$ hybridizes with poly(dA). The synthesis of the mixed sequence allows us to determine the orientation of the complementary strands in the duplex. It is observed that with α-homo-DNA and RNA, the parallel annealing gives the most stable duplexes (in contrast to hybridization of natural nucleic acids). Although an exact comparison cannot be made (due to the presence of 5-methylcytosine bases in the α-homo-oligomers) it is generally observed that the α-homo-DNA:RNA duplexes are somewhat less stable than the corresponding DNA:RNA duplexes. For example, the stability of the α-homo-DNA:RNA 12-mer (parallel) at 1 M NaCl is the same as the stability of the DNA:RNA complex (antiparallel) at the same salt concentration, although the former duplex contains seven 5-methylcytosine bases instead of the cytosine bases. Because of the different strand orientation it is not always straightforward to interpret the data. However, the DNA:RNA duplex formed between a polypyrimidine (DNA) and polypurine (RNA) strand (which is used to compare stability with α-homo-DNA containing duplexes) is more stable than the polypurine (DNA):polypyrimidine (RNA) duplex. The dsRNA complex remains the most stable association.

We also have evaluated whether the parallel duplex formed between the α-homo-DNA 12-mer and its RNA complement is susceptible to cleavage by *E. coli* RNaseH. However, we did not observe any cleavage reaction under those circumstances where a reference antiparallel DNA/RNA duplex is completely degraded (data not shown).

CD Spectral analysis: The CD spectrum was taken of the parallel hybrid formed between α-homo-DNA 12-mer (Table 2, T_m: 67 °C) and its RNA complement at 0.1 M NaCl. This spectrum is characterized by the occurrence of a negative Cotton effect at 260 nm (Figure 3). Although natural nucleic acids are hybridizing in an antiparallel way, we used them as

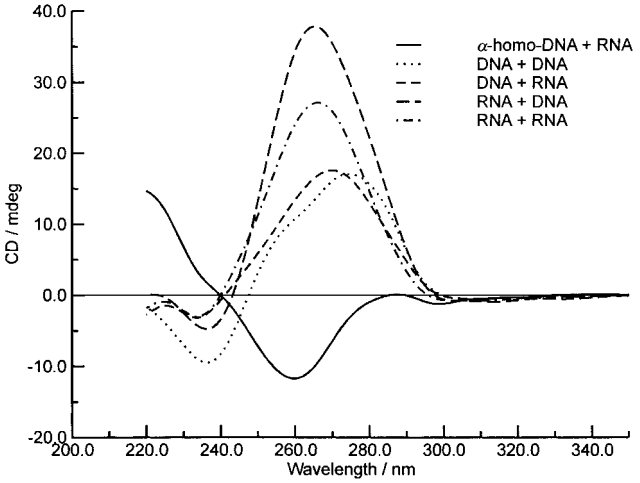

Figure 3. CD spectra of α-homo-DNA:RNA duplexes compared with the spectra of natural nucleic acids duplexes. Spectra were recorded at 10 °C (buffer 0.1 M NaCl, 0.02 M potassium phosphate at pH 7.5, and 0.1 mM EDTA) with a concentration of 4 μM of each strand.

reference for the interpretation of the spectra obtained with α-homo-DNA. Parallel or antiparallel orientation of the sugar-phosphate backbone should not induce drastic changes in the CD spectra when helix parameters remain the same. However, in order to make parallel annealing possible, it is expected that some of the helix parameters must alter and this will have its reflection on the CD signals.[40] Nevertheless, we determined the CD spectra (see Table 2 for T_m values) of the dsRNA (T_m: 72 °C), RNA:DNA (T_m: 47 °C), DNA:RNA (T_m: 64 °C), and dsDNA (T_m: 50 °C) duplexes from which the first (dsRNA) and the third (DNA:RNA) hybrids have a polypurine RNA strand, although in opposite orientation to the RNA strand of the α-homo-DNA:RNA duplex. The second (RNA:DNA) and last (dsDNA) hybrids have a DNA polypurine strand of the same sequence and orientation as the above-mentioned RNA strand. All hybrids have DNA or RNA polypyrimidine strand of the same sequence and orientation as the α-homo-DNA 12-mer. A striking difference, however, is that the RNA strands are composed of uracil/cytosine bases, the DNA strands have thymine/cytosine bases and the α-homo-DNA possesses thymine/5-methylcytosine bases. It has been described in literature that the presence of a methyl group in the major groove may affect the conformation of the oligonucleotide in solution depending on the sequence and conditions. In some cases, introduction of 5-methylcytosine does not significantly influence DNA conformation[41] while, in other cases, A to B or B to Z transitions are promoted.[42] However, as pyranoses mainly occur in one

© WILEY-VCH Verlag GmbH, D-69451 Weinheim, 2001
0947-6539/01/0723-5186 $ 17.50+.50/0 *Chem. Eur. J.* **2001**, *7*, No. 23

of the two chair conformations, we do not expect that the replacement of cytosine by 5-methylcytosine will have a drastic influence on duplex conformation (easy pseudorotation influencing local helix geometry will not take place).

The dsRNA, DNA:RNA, and RNA:DNA duplexes show a typical A-form geometry with a maximum around 260–270 nm. The CD spectrum of the dsDNA shows a positive signal at 275 nm and a negative signal at 235 nm, which is expected for a β-type structure. However, the CD spectrum of the α-homo-DNA:RNA duplex is completely different from all other reference spectra and, above 240 nm, is somewhat the mirror-image of the RNA:DNA curve. It may be concluded that the geometry of the α-homo-DNA:RNA parallel duplex is different from that of regular antiparallel nucleic acids aggregates. As the nature of the duplex cannot be extracted from these CD experiments, we compared the experimental data with those described in literature for parallel oriented α-DNA:β-DNA duplexes of related sequences.[40, 41] The CD spectra of α-CCTTCC and α-$(Tp)_7T$ are characterized by a negative band around 265 nm, while the spectra of β-CCTTCC and β-$(pT)_8$ show a positive band at a slightly higher wavelength.[40, 43] This was explained by quasi-topological enantiomeric behavior of α- and β-anomers (the α-anomer as geometric mirror image of the β-anomer with respect to a plane parallel to the sugar moiety).[43] The CD spectrum of the complex formed between α-CCTTCC and β-GGAAGG shows a negative signal at 280 nm while the CD spectrum of the duplex formed between α-GGAGG and β-CCTTCC shows a positive signal at the same wavelength. The sign of the Cotton effect is apparently dependent on the sequence and annealing mode. A comparison of the spectrum obtained of α-homo-DNA:RNA and of α-$(Tp)_7T$:oligo(rA) is difficult to make as the former is a parallel duplex and the latter is an antiparallel hybrid.[25] The data we obtained for the α-homo-DNA:RNA duplex correspond to the results described for the α-polypyrimidine-DNA:β-polypurine-DNA sequence[40] and suggest that the geometry of both duplexes is similar but not identical.

Molecular modeling: Molecular modeling has been used to obtain initial parameters for the duplex formed between α-homo-DNA and RNA. For building the model an α-homo-DNA with pyrimidine bases was used, which are identical to the oligonucleotide for which experimental T_m data are available (Table 2, α-h($TC^{Me}TC^{Me}C^{Me}TC^{Me}TC^{Me}C^{Me}C^{Me}T$). Three models were envisaged (Table 3). As hybridization experiments show that α-homo-DNA forms parallel duplexes with RNA and only very weak duplexes with DNA, model 3 (Table 3) is less likely than model 1 and model 2. Indeed, model 3 was very unstable as could be observed by computer calculations.

Table 3. The starting structures for the α-homo-DNA:RNA duplex that were considered for model building.

Model	duplex starting conformation	α-homo-DNA base orientation	RNA base orientation	Strand alignment
1	Arnott A	eq	ax	parallel
2	Arnott A	ax	ax	parallel
3	Arnott B	eq	eq	parallel

NMR experiments, X-ray diffraction, and conformational search indicate that α-homo-nucleosides with a pyrimidine base moiety preferentially occur in a $^1C_4$ conformation with an equatorially oriented base moiety. The axial conformation is about 6 to 8 kcal mol^{-1} higher in energy for one monomer unit (Table 4).

Table 4. Conformational search of 2′,3′-dideoxy-α-D-glucopyranosyl and 2′,3′-dideoxy-β-D-glucopyranosyl nucleosides: Energies [kJ mol^{-1}] of the mononucleosides (Amber, GB/SA solvent model).

Base	Thymine			Adenine		
conformation	equatorial	axial	ΔE	equatorial	axial	ΔE
α	−319	−284	35	−327	−301	26
β	−310[a]	−284[a]	26	−317	−310	7

[a] Values from ref. [70].

If the duplex would adopt an A-like conformation with the α-homo-DNA bases axially oriented, the loss in energy in going from the equatorial to the axial conformation must be compensated by stacking interactions and interstrand hydrogen bonding. Stacking and hydrogen-bond interactions could provide enough stabilization energy (stacking AG:TC −9.81 kcal mol^{-1} for a dimer in β-DNA, hydrogen bonding in GC pair −16 kcal mol^{-1} and −7.8 kcal mol^{-1} for AT pair[71]) for the chair inversion of all the pyranose nucleosides in the oligomers. Looking at the structural and energetic requirements of the α-homo-DNA for hybridization, model 1 might fit the best. Unfortunately, this model gave unstable duplexes during the molecular dynamics simulations. Model 2, starting from the Arnott A conformation, resulted at first sight into stable duplexes and we continued working with this model. During the molecular dynamics simulation, however, the helix started to unwind and became somewhat more stretched. The ultimate and penultimate α-homo-DNA monomers (at the 4′-end) changed their sugar puckering from $^4C_1$ (chair with axial base) to $^1C_4$ (chair with equatorial base) while the RNA ribose sugars remained in their C3′-*endo* puckering. After 200 ps molecular dynamics simulation, model 2 was altered and a new duplex was created having all bases in the α-homo-DNA chain equatorially oriented. Continuing molecular dynamics simulations for another 100 ps did not change this conformation. The structures during the simulation were carefully monitored for minor changes but the duplex apparently reached a stable conformation after 200 ps. The energy of the α-homo-DNA chain obtained with Amber was about 50 kcal mol^{-1} more stable than the α-homo-DNA in an initial structure from the model 2 simulation. The final model is shown in Figure 4. A close-up of one base pair showing clearly the $^1C_4$ sugar conformations of the α-homo-DNA and the C3′-endo conformation of the complementary RNA is shown in Figure 5.

The results of the curvature analysis using the Curves 5.0 program, are given in Tables 5 and 6. The analysis was done using one optimal linear axis (A Curves analysis which calculated an optimally curved axis produced a completely

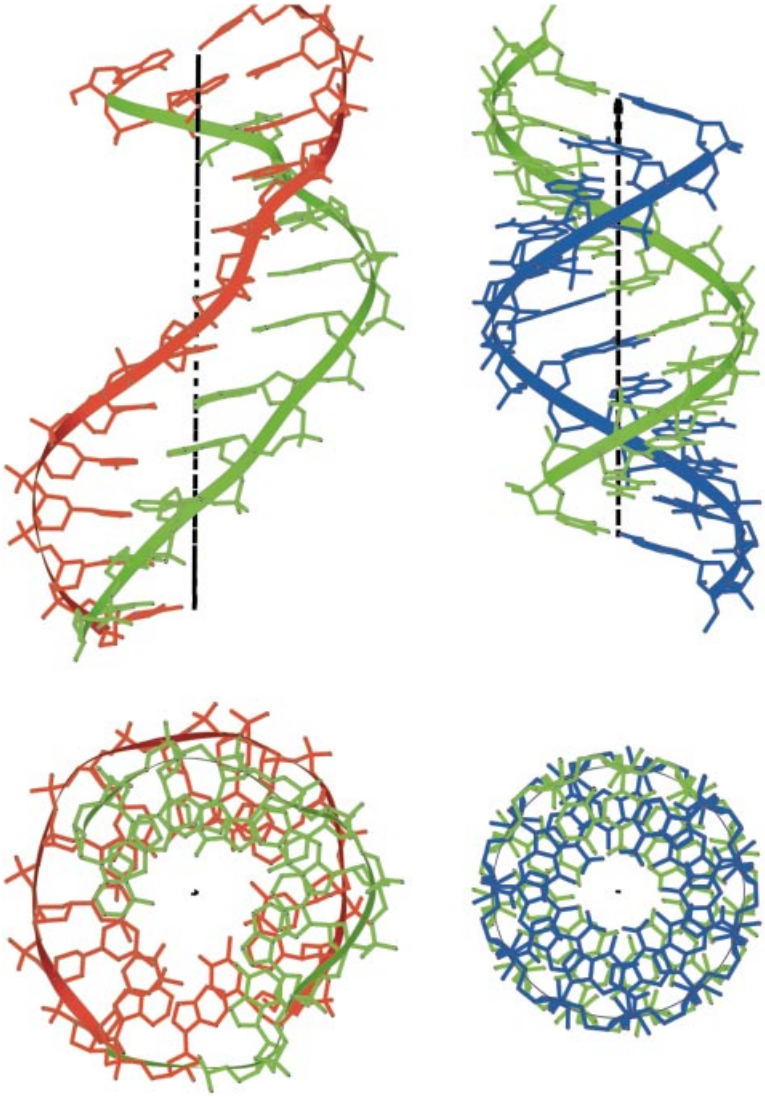

Figure 4. Top and side view of the structure of oligonucleotide hybrids composed of parallel oriented α-homo-DNA and RNA (α-TC^{Me}TC^{Me}C^{Me}TC^{Me}TC^{Me}C^{Me}C^{Me}T:r-AGAGGAGAGGGA). The α-homo-DNA nucleotides have equatorially oriented bases while the RNA chain has pseudoaxially oriented bases. For comparison purposes an ideal A-RNA helix is also shown. Pictures generated using Bobscript.[71, 72]

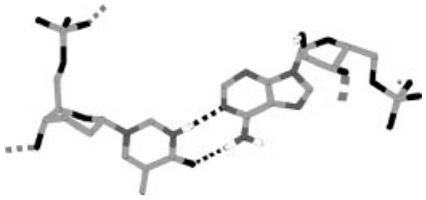

Figure 5. Three-dimensional picture of a α-h(T):r(A) nucleotide pair clearly showing the pseudoaxially oriented adenine in RNA and the equatorially oriented base in the α-homo-nucleotide.

curved axis which followed the midpoints of the base pairs but did not represented the helical symmetry.).

The average helical parameters describe a helix with base pairs displaced over 5.7 Å into the minor groove and inclined over -0.2° with respect to the helical axis. The base pairs generally show no propeller twisting (-2°). The average rise consists of 3.56 Å and the mean helical twist 24.0°, implying 15 base pairs in a full helical turn. For the local helical parameters, where the notion of a helical axis is abandoned, an average slide of 7.1 Å and an average roll of 18.0° are found. Figure 4 shows the side and top view of this double helix depicted next to the well known Arnott A-helix. It is clear that the major groove width is much larger than of regular A- or B-type duplexes.

The dihedral angles (Table 7) do not give a regular pattern. However, all dihedral angles (Tables 5, 6) except χ in the α-homo-DNA chain are closer to the torsion angles found for B-DNA right-handed helices. The torsion angles in the RNA chain are more in the ranges observed for the A-DNA right-handed helices.[45]

The sugar ring puckering parameters (Table 8) reveal that the sugar rings in the α-homo-DNA chain adopt a chair conformation slightly distorted towards the half-chair conformation (mean $\theta = 169^\circ$) with a mean puckering amplitude slightly lower than the one for an ideal cyclohexane chair conformation (0.53 Å versus 0.63 Å). The bases are positioned in an equatorial orientation. The ribose sugars have a C3′-*endo* conformation (pucker phase angle $P \approx 18^\circ$).

Closely related to the sugar puckering and the backbone torsional angles is the distance between adjacent phosphates of the same oligonucleotide chain. The different sugar puckerings as observed for the different helical types imply different intraphosphate distances. The C2′-*endo* puckering mode observed for B-type helices pushes adjacent phosphates of one chain about 7 Å apart. The C3′-*endo* puckering of the A-type helices is associated with a shorter intraphosphate distance of only 5.9 Å, giving rise to underwound helices compared with those of the B-family. The average intraphosphate distance (6.2 Å) together with the ribose C3′-*endo* puckering with axially oriented bases give the RNA strand some properties of an A-helix ($\delta = 80^\circ$ versus 83° for an A-helix). In the α-homo-DNA chain the intraphosphate distance is 6.9 Å which is more similar to a B-helix (7 Å). This can be explained by the slightly distorted chair conformation with equatorially oriented bases ($\delta = 159^\circ$ versus 157° for a B-helix). In general, however, the geometry of the duplex formed between α-homo-DNA and RNA is significantly different from A- and B-type duplexes and shows much more irregularities.

© WILEY-VCH Verlag GmbH, D-69451 Weinheim, 2001
0947-6539/01/0723-5188 $ 17.50+.50/0 *Chem. Eur. J.* **2001**, *7*, No. 23

Table 5. Helical parameters as calculated with Curves 5.0. The analysis was done making use of one optimal linear axis, part a.

Global helical parameters	Dislocation [Å]	Axial rise [Å]	Helix twist [°]	Tilt [°]	Inclination [°]	Propeller twist [°]	Minor groove width [Å]	Minor groove depths [Å]	Major groove width [Å]	Major groove depths [Å]	Interstrand P–P distance [Å]	Helical symmetry	Pitch height [Å]
rA24–α T1	6.57	1.73	22.27	10.82	−26.33	−10.30	X	X	X	X	17.11		
rG25–α C3	6.54	2.96	30.12	11.19	−15.52	−8.95	7.70	1.18	X	X	16.98		
rA26–α T5	6.32	3.92	12.52	2.61	−4.32	4.08	7.19	2.68	X	X	17.50		
rG27–α C7	5.29	3.69	29.80	2.67	−1.71	−3.20	8.40	3.04	X	X	17.48		
rG28–α C9	6.01	2.98	23.68	12.45	0.96	0.56	8.51	2.23	22.76	12.17	17.95		
rA29–α T11	6.57	4.56	20.51		−1.82	13.41	8.75	6.58	1.95	22.48	3.86	16.92	
rG30–α C13	5.84	4.66	16.36		−1.27	11.60	3.71	6.16	2.42	25.25	7.84	16.66	
rA31–α T15	4.87	3.89	26.61		−1.80	10.33	−9.47	6.51	2.74	25.86	6.96	17.72	
rG32–α C17	4.95	3.99	33.15		−8.48	8.53	7.41	6.91	2.66	X	X	17.84	
rG33–α C19	4.70	3.20	22.56	3.66	0.05		−3.43	8.20	1.30	X	X	17.97	
rG34–α C21	4.92	3.54	26.89		−6.35	3.72	−5.94	8.66	1.41	X	X	16.56	
rA35–α T23	5.34	X	X	X	−2.64	−5.88	X	X	X	X	X		
Average	5.66	3.56	24.04	2.15	−0.16	−1.89		2.16	24.09	7.71	17.34	15-1	75.7
A[a]	−5.3	2.73	32.7	17	12		11.0	2.8	2.7	13.5	5.9	11-1	30.9
B[a]	0	3.38	36.0	−2.1	2.4		5.7	7.5	11.7	8.5	7.0	11-1	33.8

[a] Values from refs. [44] and [73].

Table 6. Helical parameters as calculated with Curves 5.0. The analysis was done making use of one optimal linear axis, part b.

Local helical parameters	Slide [Å]	Roll [°]
rA24–α T1	2.59	0.34
rG25–α C3	−1.41	98.18
rA26–α T5	2.44	106.80
rG27–α C7	−1.15	−9.01
rG28–α C9	−0.83	61.40
rA29–α T11	1.61	−36.27
rG30–α C13	2.51	83.73
rA31–α T15	3.51	−72.53
rG32–α C17	−3.02	−73.53
rG33–α C19	2.99	29.53
rG34–α C21	2.77	9.78
rA35–α T23	X	X
Average	7.09	18.04
A	−2.13	8.95
B	−0.33	−0.28

NMR analysis: A preliminary NMR study on the α-homo-(TCTAAACTC):RNA complex was started to obtain experimental data verifying the modeling results. In a first stage single stranded α-homo (TCTAAACTC) was studied in D_2O. So far signals from the nine sugar moieties in the oligomer are identified using COSY,[46] TOCSY,[47] and NOESY[48] spectra in D_2O. As a starting point in the assignment strategy, the H1′ signals at $\delta = 5.6$ to 6.1 were used. Each of these anomeric protons shows a strong and a weak COSY crosspeak in the high field region between $\delta = 1.4$ to 2.5. Similar to H2′1 and H2′2 in deoxyriboses of DNA,[49], H2′1, H2′2, H3′1 and H3′2 of the non-oxygenated carbons are expected to resonate at this chemical shift. The H2′ with a strong *J* coupling to H1′, also shows a strong geminal coupling to the H2′ that is weakly coupled to H1′ and a strong coupling to one of the H3′ signals in the same high field region ($\delta = 1.4$ to 2.5). The latter H3′ has strong intraresidue NOE to H1′ and a proton signal at $\delta =$

Table 7. Dihedral angles of the α-homo-DNA strand and the RNA strand in the duplex.

α-homo-DNA	α	β	δ	ε	γ	ς	χ	RNA	α	β	δ	ε	γ	ς	χ
T	–	–	162	–	−178	–	165	**A**	–	–	74	–	45	–	−160
C^{Me}	−68	165	161	−105	42	144	136	**G**	−72	−172	73	−170	73	−68	−170
T	−68	−178	154	−158	46	−133	132	**A**	99	−172	73	−157	50	−50	−163
C^{Me}	85	−178	155	−91	−163	158	114	**G**	–	176	64	−157	−95	−68	−171
C^{Me}	−77	−166	144	179	54	−94	141	**G**	−93	179	83	−167	65	−52	−162
T	−69	−159	164	−162	17	−116	159	**A**	143	−159	78	179	55	−71	−159
C^{Me}	−85	172	158	−86	38	149	133	**G**	97	180	85	−136	−164	−68	171
T	121	−179	175	−116	−172	179	117	**A**	139	−167	81	−179	−164	−72	−150
C^{Me}	46	−163	150	−178	60	42	132	**G**	−70	−178	97	−152	−96	−63	175
C^{Me}	38	−172	159	54	57	17	157	**G**	130	180	79	−177	−172	−65	−145
C^{Me}	26	32	162	60	26	57	161	**G**	−71	−168	85	−151	62	−71	−167
T	−80	169	164	−160	32	−63	142	**A**	−163	−171	88	−160	−155	−68	−145
av	−12	169	159	193	78	162	141	**av**	203	186	80	197	139	−65	196
(sd)	(73)	(45)	(8)	(72)	(65)	(89)	(16)	**(sd)**	(80)	(7)	(8)	(13)	(84)	(7)	(13)
A	−88	−155	83	−179	54	−52	−155								
B	−46	−147	157	155	36	−96	−98								

Table 8. Sugar puckering parameters of the nucleotides.

α-homo-DNA	θ [°]	φ [°]	Q [Å]	RNA	q [Å]	P [°]
T	159.0	351.0	0.48	A	0.43	16.59
C^{Me}	176.3	178.0	0.56	G	0.48	14.09
T	160.1	334.6	0.55	A	0.46	2.59
C^{Me}	171.1	336.0	0.48	G	0.40	28.55
C^{Me}	163.0	316.5	0.48	G	0.29	13.14
T	169.7	258.9	0.48	A	0.44	18.65
C^{Me}	170.6	247.5	0.51	G	0.37	19.50
T	167.6	15.8	0.56	A	0.37	25.61
C^{Me}	175.5	196.7	0.55	G	0.40	355.06
C^{Me}	170.4	255.6	0.57	G	0.38	17.52
C^{Me}	179.4	48.5	0.57	G	0.41	352.33
T	170.7	328.9	0.55	A	0.38	10.57
av	169	239	0.53	**av**	0.40	12.85
(sd)	(6)	(107)	(0.04)	**(sd)**	(0.05)	(10.69)

4.0–4.5, which was assigned to H4′ based on the TOCSY spectrum. None of the H4′ signals showed any strong COSY crosspeaks. Using the H4′ to H5′ crosspeaks in the TOCSY spectrum, H5′ signals could be assigned. Attempts to stereospecifically distinguish H6′1 and H6′2 were unsuccessful. The one-dimensional ^{31}P spectrum showed only broad signals clustered around $\delta = 0$, hampering through bond sequential assignment of the sugar moieties by ^{1}H,^{31}P correlation spectra. Most likely, flexibility of the backbone in the single stranded oligomer is causing conformational averaging at the phosphodiester linkage resulting in a broadening of the ^{31}P NMR signals.

The data obtained on the sugar ring systems in the single stranded oligomer allow to determine the conformation of sugars in α-homo(TCTAAACTC). An asymmetric six-membered ring system theoretically has two low energy chair conformations that may interconvert through the boat and twist forms as intermediates (Figure 6). Structural data

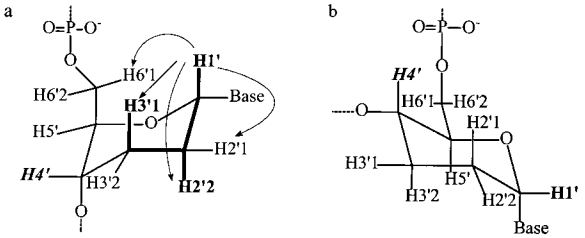

Figure 6. The two chair conformations of α-homo-DNA (a: with equatorial base moieties; b: with axial base moieties). The conformation "a" predominates in single strand α-homo(TCTAACTC) as deduced from ^{3}J values and NOE contacts.

observed by NMR are considered as the result of conformational averaging in solution.[50] Strong $^{3}J_{HH}$ coupling (≈9 Hz) of one of the H2′ to H1′ as well as to one of the H3′ is only possible when all of these protons are predominantly in a cross-diaxial position, where dihedral torsion angles between the considered protons are about 180 ± 30°. The absence of any COSY crosspeaks from H4′ signals can be explained by an equatorial position of the latter, giving rise to small $^{3}J_{H4',H5'}$, $^{3}J_{H4',H3'1}$, and $^{3}J_{H4',H3'2}$ couplings (theoretically 2–3 Hz).[51] Only a chair-like predominant conformation of the six-membered sugar ring with the base in an equatorial position, as depicted in Figure 6a, is in agreement with these experimental data. The observed intraresidue NOE contacts from H1′ to H2′1, H2′2′, H3′, and one of the H6′ protons confirm this as the major type of sugar conformation.

In the second stage of the NMR study, an equimolecular amount of a complementary RNA nonamer was added to the sample described before. The sequence of the RNA 5′-AGAUUUGAG-3′ was chosen to favor a duplex formation of α-homo(TCTAAACTC) and RNA with parallel oriented strands. One-dimensional spectra of non-exchangeable anomeric and base protons were used to monitor the degree of complex formation during the titration. At 5 °C, the ^{1}H as well as the ^{31}P NMR spectra in D_2O of the RNA:α-homo-DNA complex gave nicely resolved sharp signals, with chemical shifts clearly different from those of the single stranded oligomers; this is indicative for a strong and stable complex between both molecules at the measuring conditions (Figure 7). A one-dimensional jump-return spectrum[52] in 90 % H_2O showed several imino signals at $\delta = 10$ to 14, typical for Watson–Crick base pairing.[53] Nine different imino signals could be distinguished using a two-dimensional watergate NOESY, consistent with nine base pairs between the two parallel oriented strands.

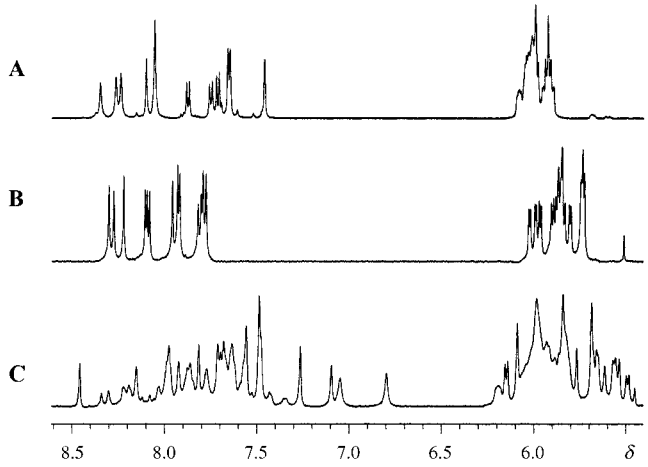

Figure 7. One-dimensional NMR spectra in D_2O of the α-homo-DNA (A) and RNA oligonucleotides (B) compared with the same spectral region of the complex (C).

Patterns from α-homo-DNA sugar proton signals in COSY, TOCSY, and NOESY spectra of the complex with RNA were very similar to those in the single stranded α-homo-DNA. Also in this sample, strong $^{3}J_{HH}$ coupling (≈9 Hz) of one of the H2′ to H1′ as well as to one of the H3′ was observed in all α-sugars. Intrasugar NOE contacts of H1′ to H2′1, H2′2, H3′1, and one of the H6′ protons, characteristic for a sugar ring in chair conformation with the base in an equatorial position, are visible in a NOESY spectrum with mixing time of 150 ms.

Ribose sugars in the RNA part of the complex behave remarkably different from the single-stranded RNA. In the latter, the H1′ signals are split by an observed $^{3}J_{H1',H2'}$ of about 5 Hz, a typical average for fast interconversion between N-type and S-type conformation with $^{3}J_{H1',H2'}$ of ≈1 Hz and

© WILEY-VCH Verlag GmbH, D-69451 Weinheim, 2001
0947-6539/01/0723-5190 $ 17.50+.50/0 *Chem. Eur. J.* **2001**, *7*, No. 23

≈10 Hz, respectively.[54] The same anomeric RNA protons in the complex with α-homo-DNA are singlets, without observable splitting from $^3J_{H1',H2'}$, characteristic for an N-type sugar conformation with $^3J_{H1',H2'}$ in the same range as the H1′ linewidth.

The molecular modeling and NMR experiments have been done with a different duplex sequence because of historical reasons. Modeling and synthesis were started at the same time but evolved differently. Yet we may conclude that, as the NMR experiments of the duplex with a more complex sequences than the modeled duplex confirm some conformational properties of the model, the overall conformation of the duplexes is, most likely, similar for both sequences.

Conclusion

Two main criteria for selecting nucleic acid alternatives as potential competitors of RNA for the generation of a genetic system, were proposed: a) a potentially natural type of molecular structure that is a sugar moiety belonging to the family of aldosugars and b) the capacity for informational base pairing in the Watson–Crick mode.[28] In these studies, β-homo-DNA was first used as artificial model for the family of hexopyranosyl oligonucleotides.[29] Later, the hydroxylated (*β-allo*, *β-altro*, *β-gluco*) analogues were synthesized and it was concluded that they could not be viable competitors of RNA because of functional reasons.[28] As demonstrated with β-homo-DNA[27] and pentopyranosyl oligomers,[55, 56] β-pyranose oligonucleotides form very stable, quasi-linear and antiparallel oriented Watson–Crick base-pairing systems. However, β-pyranose oligonucleotides do not cross-pair with natural nucleic acids which argues against their potential role as direct precursor of RNA in an evolving biological system. We investigated the hybridization properties of the isomeric oligonucleotides (α-homo-DNA) and, likewise, used the dideoxy analogues as model system. We observed that α-homo-DNA is a self-pairing system with the properties of cross-pairing with its RNA complement and less well with DNA complement, by parallel strand orientation. The base moieties in the α-homo-DNA strand are equatorially oriented and those in the RNA strand are pseudoaxially oriented (Figure 5). The geometry of the duplex is significantly different from those of existing double stranded nucleic acids and can be classified as a non-A-, non-B-type helix with an average of 15 base pairs per turn. The geometry of the duplex can be considered as intermediate between the natural A-type helix and the unnatural ladder-like structure.

In the furanose series, the α-oligonucleotides are able to hybridize with the β-nucleic acids.[8, 9]. This is, likewise, the case with locked nucleic acids where α-L-ribo-LNA (oligothymidylate) recognizes DNA and RNA (oligoadenylate).[25, 26] These results led the authors to suggest that "constitution (rather than configuration) could have been a decisive factor in an early-stage combinatorial chemical evolution of present [β-pentofuranose] nucleic acid structure".[26] In the pyranose series, configuration plays an important role in hybridization properties. While β-homo-DNA does not hybridize with natural nucleic acids, α-homo-DNA does. Previously, cross-pairing capability of α-L-lyxopyranosyl (3′→4′) oligonucleotides with DNA was observed, although the nature of the hybridization mode was described by the author as "capriciously".[28] Explanations for the emergence of RNA as a dominant player in the origin of life are based on its selection either by combinatorial generation and functional selection, either by synthetic contingency or as the result of an evolving biological system that later became extinct.[57] One possibility for this last hypothesis is that furanose nucleic acids evolved from pyranose nucleic acids. The former polymers have more conformational diversity, which might be important for evolution and transfer of information. The pyranose nucleic acids might have been a predecessor of the furanose nucleic acids, but then became extinct because of functional criteria. We demonstrate here that informational base pairing is possible between α-homo-DNA and RNA. The α-homo-DNA remains an artificial model and the data obtained should be confirmed for α-glucose-DNA. A strong argument against an evolutionary pathway involving α-glucose-DNA is the absence of a role for the product of the thermodynamically controlled aldolization (β-pyranoses) in favor of a compound formed by kinetically controlled reaction (α-pyranoses). Although it may be hypothesized that α-glucose nucleotides may have been "an element of a kinetically labile reaction library possessing informational capacity and with the potential to evolve to constitutionally more robust variants in which the information is preserved",[58] it now seems clear (based on this and previous work with hexopyranose oligonucleotides) that hexopyranose DNA was, most likely, not a direct precursor of our contemporary nucleic acids. Arguments why hexopyranose nucleic acids failed as RNA competitors have been previously discussed.[28]

Experimental Section

General methods: UV spectra were recorded with a Philips PU8740 UV/Vis or Uvikon 940 spectrophotometer. The ^{1}H and ^{13}C NMR spectra were recorded with a Varian Gemini 200 or Unity 500 spectrometer. Tetramethylsilane (TMS) was used as internal standard for the ^{1}H NMR spectra (s = singlet, d = doublet, t = triplet, m = multiplet), and the center peak of the solvent $CDCl_3$ ($\delta = 77.0$) for the ^{13}C NMR spectra. Mass spectrometry measurements were obtained using a Kratos Concept IH mass spectrometer with liquid secondary ion mass spectrometry (LSIMS) ionization. NPOE (2-nitrophenyl octyl ether) was used as the matrix. Exact mass measurements were performed on a quadrupole/orthogonal-acceleration time-of-flight (Q/oaTOF) tandem mass spectrometer (qTof2, Micromass, Manchester, UK) equipped with a standard electrospray ionization (ESI) interface. Samples were infused in a 2-propanol/water 1:1 mixture at 3 μL min^{-1}. Pyridine was heated under reflux overnight on potassium hydroxide and distilled. Dichloromethane was stored on calcium hydride, refluxed, and distilled. Precoated Macherey–Nagel Alugram SIL G/UV 254 plates were used for thin-layer chromatography (TLC) and products were visualized with UV light. Column chromatography was performed on Acros Organics silica gel (0.2–0.5 mm, pore size 4 nm).

6′-*O*-Monomethoxytritylation of the α-D-homo nucleosides

Reactions were carried out on a 1 mmol scale using 1.1 equivalents of monomethoxytrityl chloride in dry pyridine (10 mL) at room temperature overnight. After addition of a saturated $NaHCO_3$ solution (1 mL), the reaction mixture was evaporated, diluted with CH_2Cl_2 (30 mL), and washed with H_2O (3 × 30 mL). The organic layer was dried, evaporated and the 6′-*O*-monomethoxytritylated nucleoside was purified by column chromatog-

raphy (hexane/EtOAc 2:8 for thymine; hexane/EtOAc 5:5 for 5-methylcytosine; CH_2Cl_2/MeOH 98:2 for cytosine), except for the adenine analogue which was purified by preparative TLC (EtOAc/toluene/MeOH 95:5:1).

1-(6-*O*-Monomethoxytrityl-2,3-dideoxy-α-D-*erythro*-hexopyranosyl)-thymine (55%): exact mass calcd for $C_{31}H_{32}N_2O_6Na$ $[M+Na]^+$: 551.2158, found 551.2142.

1-(6-*O*-Monomethoxytrityl-2,3-dideoxy-α-D-*erythro*-hexopyranosyl)-5-methyl-N^4-benzoylcytosine (50%): exact mass calcd for $C_{38}H_{38}N_3O_6$ $[M+H]^+$: 632.2760, found 632.2774.

1-(6-*O*-Monomethoxytrityl-2,3-dideoxy-α-D-*erythro*-hexopyranosyl)-N^4-benzoylcytosine (50%): exact mass calcd for $C_{37}H_{36}N_3O_6$ $[M+H]^+$: 618.2603, found 618.2604.

1-(6-*O*-Monomethoxytrityl-2,3-dideoxy-α-D-*erythro*-hexopyranosyl)-N^6-benzoyladenine (67%): exact mass calcd $C_{38}H_{36}N_5O_5$ $[M+H]^+$: 642.2716, found 642.2717.

The ^{1}H NMR and ^{13}C NMR spectra are collected in Table 9.

Oligonucleotide synthesis

Analytical details for the phosphoramidite building blocks are as follows:

1-(6-*O*-Monomethoxytrityl-4-*O*-[*N*,*N*-diisopropyl(2-cyanoethyl)phosphoramidite-2,3-dideoxy-α-D-glucopyranosyl)-thymine: R_f (hexane/acetone/TEA 49:49:2) = 0.45; exact mass calcd for $C_{40}H_{50}N_4O_7P$ $[M+H]^+$: 729.3417, found 729.3422; ^{31}P NMR: δ = 148.63, 148.47.

1-(6-*O*-Monomethoxytrityl-4-*O*-[*N*,*N*-diisopropyl(2-cyanoethyl)phosphoramidite-2,3-dideoxy-α-D-glucopyranosyl)-N^4-benzoylcytosine: R_f (hexane/acetone/TEA 49:49:2) = 0.47; exact mass calcd for $C_{46}H_{53}N_5O_7P$ $[M+H]^+$: 818.3682, found 818.3663; ^{31}P NMR: δ = 148.64, 148.61.

1-(6-*O*-Monomethoxytrityl-4-*O*-[*N*,*N*-diisopropyl(2-cyanoethyl)phosphoramidite-2,3-dideoxy-α-D-glucopyranosyl)-N^4-benzoyl-5-methylcytosine: R_f (hexane/acetone/TEA 49:49:2) = 0.61; LSIMS (NPOE): m/z: 832 $[M+H]^+$.

9-(6-*O*-Monomethoxytrityl-4-*O*-[*N*,*N*-diisopropyl(2-cyanoethyl)phosphoramidite-2,3-dideoxy-α-D-glucopyranosyl)-N^6-benzoyl adenine: R_f (hexane/acetone/TEA 49:49:2) = 0.32; exact mass calcd for $C_{47}H_{53}N_7O_6P$: $[M+H]^+$: 842.3795, found 842.3790; ^{31}P NMR: δ = 148.65, 148.23.

Oligonucleotide synthesis was carried out on an automated DNA synthesizer with the phosphoramidite approach, model ABI 392 (Applied BioSystems). Condensations were run at 0.12 M of the respective modified building blocks for 10 min to ensure adequate coupling yields. The sequences obtained were deprotected and cleaved from the solid support by treatment with concentrated ammonia at 55 °C for 16 h. After a first purification on a NAP-10 column (Sephadex G-25-DNA grade), a mono-QHR 10/10 anion-exchange column/Pharmacia) was used with the following gradient system: A) NaOH, pH 12.0 (10 mM), NaCl (0.1 M); B) NaOH, pH 12.0 (10 mM), NaCl (0.9 M). The low-pressure liquid chromatography system consisted of a Merck – Hitachi L6200A Intelligent pump, a Mono-Q HR 10/10 column, a Uvicordu SII2138 UV detector (Pharmacia-LKB) and a recorder. Product-containing fractions were immediately neutralized by addition of aqueous ammonium acetate. Following concentration, the eluent was desalted on a NAP 10 column and lyophilized.

UV-melting experiments and thermodynamic data: UV-melting experiments were recorded with a Uvikon 940 or a Carry 100 Bio spectrophotometer. Samples were dissolved in a buffer solution containing NaCl (0.1 or 1 M), potassium phosphate (0.02 M, pH 7.5) and EDTA (0.1 mM). The oligomer concentration was determined by measuring the absorbancy at 80 °C in pure water and assuming extinction coefficients in the denaturated state as used for natural DNA. The concentration in all experiments was 4 μM of each strand. Cuvettes were kept at a constant temperature with water circulating through the cuvette holder and with a thermistor immersed directly in the cuvette. For the melting experiments, temperature control and data acquisitions were carried out automatically with an IBM/PC AT-compatible computer. The samples were heated and cooled at a rate of 0.2 °C min^{-1} with data sampling every 30 s. T_m values were determined from the maximum of the first derivative curve.

CD spectra: CD spectra were measured at 10 °C with a Jasco 600 spectropolarimeter in thermostatically controlled 1 cm cuvettes corrected with a Lauda RCS 6 bath. The oligomers were dissolved and analyzed in buffer containing NaCl (0.1 M), potassium phosphate (0.02 M, pH 7.5) and EDTA (0.1 mM) and at a concentration of 4 μM of each strand.

Mass spectrometric analysis of oligonucleotides: Oligonucleotides were purified by RP HPLC on a C18 column prior to mass spectrometric analysis. A linear gradient of A: ammoniumbicarbonate (25 mM in H_2O, pH 7.0) and B: acetonitrile (80% in H_2O) was applied. Mass spectra were acquired in negative ionization mode on a quadrupole/orthogonal-acceleration time-of-flight (Q/oaTOF) tandem mass spectrometer (qTof 2, Micromass, Manchester, UK) equipped with a standard electrospray ionization (ESI) interface. Samples were infused in acetonitrile/water 1:1 at 3 μL min^{-1}. Collisionally activated dissociation (CAD) was performed with argon in the collision cell and a collision energy of 150 eV.

Model building

Conformational search: The model building and conformational analysis of the α-homo-DNA monomer was done using Macromodel 5.0.[59] The

Table 9. NMR data for 6-*O*-monomethoxytrityl-2,3-dideoxy-α-D-*erythro*-hexopyranosyl nucleosides (coupling constants in Hz).[a, b]

	B	T		C^{5Me}-N^4-Bz		C-N^4-Bz		A-N^6-Bz		
Pos	^{1}H	^{13}C	^{1}H	^{13}C	^{1}H	^{13}C		^{1}H	^{13}C	
1′	5.760 (dd, J = 2.9/9.9)	79.34	5.796 (dd, J = 2.5/9.5)	79.43	5.787 (dd, J = 3.4/9.3)	80.70	6.056 (t, J = 4.4)		75.36	
2′	1.70 – 2.15 (m)	24.25	1.75 – 2.15 (m)	24.40	2.12 (m)	24.83	2.98 (m), 2.10 (m)		25.44	
3′		25.95		25.98	1.75 – 1.95 (m)	26.07	218 (m), 1.75 (m)		26.79	
4′	3.881 (m, ΣJ = 10)	64.31	3.893 (m, J = 10)	64.31	3.908 (dt, J = 3.4/3.9)	64.66	3.795 (dt, J = 5.5/10.0)		66.98	
5′	4.103 (dd, J = 17)	78.21	4.136 (m, J = 16)	78.79	4.155 (dt, J = 3.9/6.3)	79.12	3.604 (q, J = 7.6)		79.97	
6′	3.456 (dd, J = 5.7/9.9); 3.317 (dd, J = 7.0/9.9)	62.28	3.452 (dd, J = 5.7/9.9); 3.321 (dd, J = 7.0/9.9)	62.28	3.484 (dd, J = 5.9/9.8); 3.362 (dd, J = 6.8/9.8)	62.52	3.471 (dd, J = 5.5/10.0); 3.417 (dd, J = 6.0/10.0)		64.31	
N^4	8.65 (br)	–	8.36 (br)	–	8.79 (br)	–		9.44 (br)	–	
5-Me	1.922 (d, J = 1.1)	12.38	2.115 (d, J = 1.2)	13.48	–	–	[5]	–	123.22	
5	–	110.84	–	111.84	7.252 (d, J = 7.3)	96.45	[8]	8.249 (s)	141.83	
6	–	135.82	8.310 (s)	136.97	8.135 (d, J = 7.3)	144.80	[4]	–	149.75	
2	–	149.96	–	147.72	–	154.04	[2]	8.780 (s)	152.60	
4	–	163.71	–	147.72	–	162.07	[6]	–	151.72	

[a] The resonances for the protecting groups are omitted for clarity: [f.e. for B = C-N^4-Bz: ^{1}H: a) MMTr: 3.800 (s, 3H), 68.48 (d, 2H), 7.20 – 7.45 (m, 12H); b) Bz: 7.48 (t, 2H), 7.60 (t, 1H), 7.89 (d, 2H); ^{13}C: a) MMTr: 55.25, 87.01, 113.30 (2), 127.13 (2), 127.96 (4), 128.29 (4), 130.30 (2), 135.02, 143.87 (2), 158.74. b) Bz: 127.54 (2), 129.01 (2), 133.23, 133.13, 166.7. [b] For B = C-N^4-Bz, all assignments were checked by 2D-COSY and 6 HSQC experiments on a Unity 500 spectrometer.

© WILEY-VCH Verlag GmbH, D-69451 Weinheim, 2001
0947-6539/01/0723-5192 $ 17.50+.50/0 *Chem. Eur. J.* **2001**, *7*, No. 23

building and molecular dynamics simulation of the polymer duplexes was done using midasplus[60] and Amber 4.1.[61]

Charge and force field parameter development: The force field parameters and partial charges for RNA were taken from the Amber 4.1 force field parameter database.[62] The force field parameters for the α-D-glucose sugar were taken from Amber 4.1 without modification. Some missing angle and improper torsion parameters and force constants for the 5-Me-Cytosine base were taken from comparable angles from the Amber 4.1 force field. Partial atomic charges of the α-homo-DNA nucleotide were obtained by a two-stage fitting procedure (RESP)[63] of the charges to the 6-31G* derived electrostatic potential from a Gamess calculation.[64]

Duplexes: The building and molecular dynamics simulation of the polymer duplexes was done using Midasplus[60] and Amber 4.1.[62] The α-homo-DNA:RNA parallel duplex (α-TC^{Me}TC^{Me}C^{Me}TC^{Me}TC^{Me}C^{Me}C^{Me}T:r-AGAGGAGAGGGA) was built starting from a 12-mer Arnott A-type antiparallel double RNA helix (A:U and G:C^{Me} base pairs) (model 1 and 2) and starting from a twelvemer Arnott B-type double stranded DNA helix (model 3). The duplexes were soaked in a rectangular box of explicit TIP3P water molecules[65] and 22 Na^+ counterions. After equilibration, the molecular dynamics simulation was started (with particle mesh Ewald conditions,[66] initial box size $69.3 \times 47.7 \times 48.5$ Å^3; total number of atoms is 13951) to verify the stability of the model structures.

Calculation of structural parameters: *Curvature*: The curvature analysis was done using the Curves 5.0 program.[67] The analysis was done making use of one optimal linear axis.

Sugar puckering parameters: The puckering parameters of the six-membered hexopyranose rings were calculated according to Cremer and Pople.[68] The ribose puckering parameters were calculated following Altona and Sundaralingam.[69]

NMR sample preparation and NMR spectrometry of oligonucleotides

Sample preparation: Oligonucleotide strands were dissolved in D_2O and the pD was adjusted to 7. The RNA solution (OD = 68) was titrated with the complementary α-homo-DNA solution to obtain an equimolar mixture. After adding each aliquot of the α-homo-DNA solution, the mixture was briefly heated to 80 °C and slowly cooled to room temperature to allow for duplex formation. The degree of complex formation was monitored by one dimensional proton NMR. After reaching the 1:1 RNA:α-homo-DNA titration point the sample was lyophilized and dissolved in 0.75 mL D_2O yielding a 1.2 mM duplex solution. For measurements in H_2O, the sample was lyophilized and dissolved in a 0.75 mL 90% H_2O/10% D_2O mixture.

NMR spectrometry: NMR spectra were recorded on a Varian 500 Unity spectrometer operating at 499.505 MHz. Quadrature detection was achieved by States–Haberkorn hypercomplex mode.[74] Spectra were processed using Vnmr software package (Varian).

For samples in H_2O one dimensional spectra in were recorded using a jump-return observation pulse.[52] A two dimensional of α-homo-DNA:RNA sample in H_2O was recorded at 5 °C with a 150 ms mixing time using the watergate sequence,[75] with a sweep width of 11000 Hz in both dimensions. The spectrum was recorded with 64 scans for each FID and 4096 data points in t_2 and 512 FIDs in t_1.

The two-dimensional DQF-COSY,[46] TOCSY,[47] and NOESY[48] spectra of the α-homo-DNA and α-homo-DNA:RNA samples dissolved in D_2O were recorded with a spectral width of 4200 Hz in both dimensions. DQF-COSY spectra were recorded with 4096 data points in t_2 and 400 increments in t_1. For the TOCSY experiment, a Clean MLEV17[76] was used during the 65 ms mixing time. The spectrum was acquired with 32 scans, 4096 data points in t_2 and 512 FIDs in t_1. The NOESY spectra were recorded with mixing times of 150 and 300 ms. Each experiment had 32 scans for each FID, 2048 datapoints in t_2 and 256 increments in t_1. All two-dimensional spectra data were apodized with a shifted sine bell squared function in both dimensions.

Acknowledgements

Authors thank G. Schepers for synthesis of oligonucleotides and determination of T_m values. We are indebted to Chantal Biernaux for nice editorial help. This research was supported by a grant from the K.U. Leuven (GOA 97/11).

[1] R. Bonnett, *Chem. Rev.* **1963**, *63*, 573–605.
[2] K. Suzuki, H. Nakano, S. Suzuki, *J. Biol. Chem.* **1967**, *242*, 3319–3325.
[3] F. Dinglinger, P. Renz, *Hoppe-Seylers's Physiol. Chem.* **1971**, *352*, 1157–1161.
[4] W. D. Fuller, R. A. Sanchez, L. E. Orgel, *J. Mol. Biol.* **1972**, *67*, 25–33.
[5] A. Holý, *Collect. Czech Chem. Commun.* **1972**, *38*, 100–114.
[6] U. Séquin, *Helv. Chim. Acta* **1974**, *57*, 68–81.
[7] U. Séquin, *Specialia* **1973**, 1059–1062.
[8] F. Morvan, B. Rayner, J.-L. Imbach, M. Lee, J. A. Hartley, D.-K. Chang, W. Lown, *Nucleic Acids Res.* **1987**, *15*, 7027–7044.
[9] N. G. Thuong, U. Asseline, V. Roig, M. Takasugi, C. Hélène, *Proc. Natl. Acad. Sci. USA* **1987**, *84*, 5129–5133.
[10] C. Gagnor, J.-R. Betrand, S. Thenet, M. Lemaître, F. Morvan, B. Rayner, C. Malvy, B. Lebleu, J.-L. Imbach, C. Paoletti, *Nucleic Acids Res.* **1987**, *15*, 10419–10437.
[11] C. Gagnor, B. Rayner, J.-P. Leonetti, J.-L. Imbach, B. Lebleu, *Nucleic Acids Res.* **1989**, *17*, 5107–5114.
[12] C. Thibaudeau, A. Földesi, J. Chattopadhyaya, *Tetrahedron* **1998**, *54*, 1867–1900.
[13] G. Lancelot, J.-L. Guesnet, V. Roig, N. T. Thuong, *Nucleic Acids Res.* **1987**, *15*, 7531–7547.
[14] W. H. Gmeiner, B. Rayner, F. Morvan, J.-L. Imbach, J.-W. Lown, *J. Biomol. NMR* **1992**, *2*, 275–288.
[15] C. Boiziau, R. Kurfurst, C. Cazenave, V. Roig, N. T. Thuong, J.-J. Toulmé, *Nucleic Acids Res.* **1991**, *19*, 1113–1119.
[16] F. Morvan, H. Porumb, G. Degols, I. Lefebvre, A. Pompon, B. S. Sproat, B. Rayner, C. Malvy, B. Lebleu, J.-L. Imbach, *J. Med. Chem.* **1993**, *36*, 280–287.
[17] O. Zelphati, J.-L. Imbach, N. Signoret, G. Zon, B. Rayner, L. Leserman, *Nucleic Acids Res.* **1994**, *22*, 4307–4314.
[18] M. Bolli, P. Lubini, C. Leumann, *Helv. Chim. Acta* **1995**, *78*, 2077–2096.
[19] S. Peyrottes, J.-J. Vasseur, J.-L. Imbach, B. Rayner, *Tetrahedron Lett.* **1996**, *37*, 5869–5872.
[20] A. Laurent, M. Naval, F. Debart, J.-J. Vasseur, B. Rayner, *Nucleic Acids Res.* **1999**, *27*, 4151–4159.
[21] K. Pongracz, S. M. Gryaznov, *Nucleic Acids Res.* **1998**, *26*, 1099–1106.
[22] F. Debart, A. Meyer, J.-J. Vasseur, B. Rayner, *Nucleic Acids Res.* **1998**, *26*, 4551–4556.
[23] F. Morvan, J. Zeidler, B. Rayner, *Tetrahedron* **1998**, *54*, 71–82.
[24] P. Nielsen, J. K. Dalskov, *Chem. Commun.* **2000**, 1179–1180.
[25] V. K. Rajwanshi, A. E. Hakansson, B. M. Dahl, J. Wengel, *Chem. Commun.* **1999**, 1395–1396.
[26] V. K. Rajwanshi, A. E. Hakansson, R. Kumar, J. Wengel, *Chem. Commun.* **1999**, 2073–2074.
[27] S. J. Sun, J.-C. François, C. Lavery, T. Saison-Behmoaras, T. Montenay-Garestier, N. T. Thuong, C. Hélène, *Biochemistry* **1988**, *27*, 6039–6045.
[28] A. Eschenmoser, *Science* **1999**, *284*, 2118–2124.
[29] J. Hunziker, H.-J. Roth, M. Böhringer, A. Giger, U. Diederichsen, M. Göbel, R. Krishnan, B. Jaun, C. Leumann, A. Eschenmoser, *Helv. Chim. Acta* **1993**, *76*, 259–353.
[30] K. Augustijns, A. Van Aerschot, C. Urbanke, P. Herdewijn, *Bull. Soc. Chim. Belg.* **1992**, 119–129.
[31] P. Herdewijn, H. De Winter, B. Doboszewski, I. Verheggen, K. Augustijns, C. Hendrix, T. Saison-Behmoaras, C. De Ranter, A. Van Aerschot, *ACS Symposium Series*: *Carbohydrate Modifications in Antisense Research*, *Vol. 58*, **1994**, pp. 80–99.
[32] H. De Winter, N. M. Blaton, O. M. Peeters, C. J. De Ranter, A. Van Aerschot, P. Herdewijn, *Acta Crystallogr. Sect. C* **1991**, *47*, 838–842.
[33] H. De Winter, E. Lescrinier, A. Van Aerschot, P. Herdewijn, *J. Am. Chem. Soc.* **1998**, *120*, 5381–5394.
[34] Y. Maurinsh, H. Rosemeyer, R. Esnouf, J. Wang, G. Ceulemans, E. Lescrinier, C. Hendrix, R. Busson, F. Seela, A. Van Aerschot, P. Herdewijn, *Chem. Eur. J.* **1999**, *5*, 2139–2150.
[35] P. Herdewijn, *Liebigs Annalen* **1996**, 1337–1348.
[36] G. W. Ashley, *J. Am. Chem. Soc.* **1992**, *114*, 9731–9736.
[37] M. Böhringer, H.-J. Roth, J. Hunziker, M. Göbel, R. Krishnan, A. Giper, B. Schweizer, J. Schreiber, C. Leumann, A. Eshenmoser, *Helv. Chim. Acta* **1992**, *75*, 1416–1477.
[38] G. S. Ti, B. L. Gaffney, R. A. Jones, *J. Am. Chem. Soc.* **1982**, *104*, 1316–1319.

[39] R. Busson, L. Kerremans, A. Van Aerschot, M. Peeters, N. Blaton, P. Herdewijn, *Nucleosides Nucleotides* **1999**, *18*, 1079 – 1082.
[40] J. Paoletti, D. Bazile, F. Morvan, J.-L. Imbach, C. Paoletti, *Nucleic Acids Res.* **1989**, *17*, 2693 – 2704.
[41] G. T. Walker, *Nucleic Acids Res.* **1988**, *16*, 3091 – 3099.
[42] S. Uesugi, H. Miyashiro, K. Tomita, M. Ikehara, *Chem. Pharm. Bull.* **1986**, *34*, 51 – 60.
[43] M. Durand, J. C. Maurizot, N. T. Thuong, C. Hélène, *Nucleic Acids Res.* **1988**, *16*, 5039 – 5053.
[44] W. Saenger, *Principles of Nucleic Acids Structure*, Springer, New York, **1984**.
[45] B. Schneider, S. Neidle, H. M. Berman, *Biopolymers* **1997**, *42*, 113 – 124.
[46] M. Rance, O. W. Sørensen, G. Bodenhausen, G. Wagner, R. R. Ernst, K. Wüthrich, *Biochem. Biophys. Res. Commun.* **1983**, *117*, 479 – 485.
[47] A. Bax, D. G. Davis, *J. Magn. Reson.* **1985**, *65*, 355 – 366.
[48] J. Jeener, B. H. Meier, P. Bachmann, R. R. Ernst, *J. Chem. Phys.* **1979**, *71*, 4546 – 4553.
[49] S. S. Wijmenga, B. N. M. Buuren, *Prog. Nucl. Magn. Reson. Spectrosc.* **1998**, *32*, 287 – 387.
[50] J. N. S. Evans, *Biomolecular NMR spectroscopy*, Oxford University Press, **1995**.
[51] C. A. G. Haasnoot, *J. Am. Chem. Soc.* **1992**, *114*, 882 – 887.
[52] P. Plateau, M. Guéron, *J. Am. Chem. Soc.* **1982**, *104*, 7310 – 7311.
[53] K. Wütrich, *NMR of Proteins and Nucleic Acids*, Wiley, USA, **1986**.
[54] S. S. Wijmenga, M. W. Mooren, C. W. Hilbers, in *NMR of Macromolecules*: *A Practical Approach* (Ed.: G. Roberts), Oxford University Press, Oxford, **1993**, pp. 217 – 288.
[55] I. Schlönvogt, S. Pitsch, C. Lesueur, A. Eschenmoser, B. Jaun, R. M. Wolf, *Helv. Chim. Acta* **1996**, *79*, 2316 – 2345.
[56] S. Pitsch, S. Wendeborn, B. Jaun, A. Eschenmoser, *Helv. Chim. Acta* **1993**, *76*, 2161 – 2183.
[57] M. Beier, F. Reck, R. Krishnamurthy, A. Eschenmoser, *Science* **1999**, *283*, 699 – 703.
[58] K.-U. Schöning, P. Scholz, S. Guntha, X. Wu, R. Krishnamurthy, A. Eschenmoser, *Science* **2000**, *290*, 1347 – 1351.
[59] F. Mohamadi, N. G. J. Richards, W. C. Guida, R. Liskamp, M. Lipton, C. Caufield, C. Chang, T. Hendrickson, W. C. Still, *J. Comput. Chem.* **1990**, *11*, 440 – 467.
[60] T. E. Ferrin, C. C. Huang, L. E. Jarvis, R. Langridge, *J. Mol. Graphics* **1988**, *6*, 13 – 27; T. E. Ferrin, C. C. Huang, L. E. Jarvis, R. Langridge, *J. Mol. Graphics* **1988**, *6*, 36 – 37.
[61] S. J. Weiner, P. A. Kollman, D. T. Nguyen, D. A. Case, *J. Comput. Chem.* **1986**, *7*, 230 – 252.
[62] W. D. Cornell, P. Cieplak, C. I. Bayly, I. R. Gould, K. M. Merz, D. M. Ferguson, D. C. Spellmeyer, T. Fox, J. W. Caldwell, P. A. Kollman, *J. Am. Chem. Soc.* **1995**, *117*, 5179 – 5197.
[63] C. I. Bayly, P. Cieplak, W. D. Cornell, P. A. Kollman, *J. Phys. Chem.* **1993**, *97*, 10269 – 10280.
[64] M. W. Schmidt, K. K. Baldridge, J. A. Boatz, S. T. Elbert, G. S. Gordon, J. H. Jensen, S. Koseki, N. Matsunaga, K. A. Nguyen, S. Su, T. L. Windus, M. Dupuis, J. A. Montgomery, *J. Comput. Chem.* **1993**, *14*, 1347 – 1363.
[65] W. Jorgensen, J. Chandrasekar, J. Madura, R. Impey, M. Klein, *J. Chem. Phys.* **1983**, *79*, 926 – 935.
[66] U. Esman, L. Perera, M. L. Berkowitz, T. Darden, H. Lee, L. G. J. Pedersen, *Chem. Phys.* **1995**, *103*, 8577 – 8593.
[67] R. Lavery, H. Sklenar, *J. Biomol. Struct. Dyn.* **1989**, *6*, 655 – 667.
[68] D. Cremer, J. A. Pople, *J. Am. Chem. Soc.* **1975**, *97*, 1354 – 1358.
[69] C. Altona, M. Sundaralingam, *J. Am. Chem. Soc.* **1972**, *94*, 8205 – 8212.
[70] T. Ostrowski, B. Wroblowski, R. Busson, J. Rozenski, E. De Clercq, M. S. Bennett, J. N. Champness, W. C. Summers, M. R. Sanderson, P. Herdewijn, *J. Med. Chem.* **1998**, *41*, 4343 – 4353.
[71] P. J. Kraulis, *J. Appl. Crystallogr.* **1991**, *24*, 946 – 950.
[72] R. E. Esnouf, *J. Mol. Graphics* **1997**, *15*, 132 – 134.
[73] V. A. Bloomfield, D. M. Crothers, I. Tinoco, *Nucleic Acids*: *Structures, Properties and Functions*, University Science Books, Sausalito, **2000**.
[74] D. J. States, R. A. Haberkorn, D. J. Ruben, *J. Magn. Reson.* **1982** *48*, 286 – 292.
[75] M. Piotto, V. Saudek, V. J. Sklenar, *Biomol. NMR* **1992**, *2*, 661 – 665.
[76] C. Griesinger, G. Otting, K. Wüthrich, *J. Am. Chem. Soc.* **1988**, *110*, 7870 – 7872.

Received: June 1, 2001 [F3308]

 © WILEY-VCH Verlag GmbH, D-69451 Weinheim, 2001 0947-6539/01/0723-5194 $ 17.50+.50/0